Evaluation of axial SRM for electric vehicle application

M'Hamed Belhadi, Guillaume Krebs, Claude Marchand, Hala Hannoun, Xavier Mininger

Evaluation of axial SRM for electric vehicle application

M'Hamed Belhadi[*+1], Guillaume Krebs[*], Claude Marchand[*], Hala Hannoun[+] and Xavier Mininger[*]

[*]: GeePs, Group of electrical engineering Paris

UMR CNRS 8507, CentraleSupélec, Univ Paris-Sud, Sorbonne Universités, UPMC Univ Paris 06

3, 11 rue Joliot-Curie, Plateau de Moulon F-91192 Gif-sur-Yvette CEDEX

[+]: Renault, 1 avenue du Golf, 78288 Guyancourt, France

mhbelhadi@yahoo.fr, guillaume.krebs@geeps.centralesupelec.fr

Abstract: In this paper, a study on an Axial Switched Reluctance Motor (ASRM) is provided and comparisons with an equivalent Radial Switched Reluctance Motor (RSRM) are established. A 3D Finite Element (FE) model is used for the ASRM and only 2D FE model for the radial one in order to reduce the computation time. First, a bibliographic review and descriptions of the two motors are given. Secondly, comparisons between both structures are proposed including flux linkages, developed torques, masses, torque-speed curves and cartography of minimum torque ripples. In order to make the comparisons more reliable, optimized control parameters and full operating range for electric vehicle (EV) power train are taken into account.

***Index Terms*— Switched reluctance motor, axial flux, finite element, torque-speed curve, torque ripples, EV powertrain.**

1. INTRODUCTION

The switched reluctance motor is well known for its many advantages, such as simple

[1] Corresponding author (mhbelhadi@yahoo.fr)

manufacturing, robustness, easy maintenance, good efficiency, operating in extreme conditions, no need to use magnets and low cost. All these advantages make this structure a serious and an attractive challenger for the electric vehicles traction. However, this motor presents two major drawbacks: a high torque ripples and an undesirable acoustic noise due to the stator vibrations caused by magnetic forces on stator teeth.

Depending on the magnetic flux path in the airgap, two structures of SRM can be considered: the radial SRM and the axial SRM (Fig. 1). The second one could be a solution to limit the last mentioned drawback. Indeed, for the ASRM, the radial efforts, which are perpendicular to the rotation axis, are insignificant and vibrations that originate from these efforts, should be more easily mitigable. Previous studies on ASRM highlighted some advantages such as: adjustable airgap, suitable for applications where the ratio length/diameter is low, simple cooling and simple process of lamination [1].

In order to choose the appropriate structure for electric traction, comparisons between axial and radial SRM are essentially presented. Except some works like [2]–[4], the majority of studies on switched reluctance motor for an electric traction has been made by considering a radial structure [5]–[13]. Therefore, this work focuses on the axial structure for an automobile application. Two conversion models, from one structure to another one, have been developed and the comparisons are then performed by considering specifications of electric vehicle motorization. Furthermore, the two structures are always independently studied because of their geometrical differences. This is not the case of this work, where both are studied at the same time.

2. AXIAL SRM

The ASRM is a switched reluctance motor where the magnetic field lines in the airgap are parallel to the rotation axis of the machine (Fig. 1.b). In the RSRM airgap, these lines are perpendicular to the machine axis (Fig. 1.a).There are three main ASRM categories.

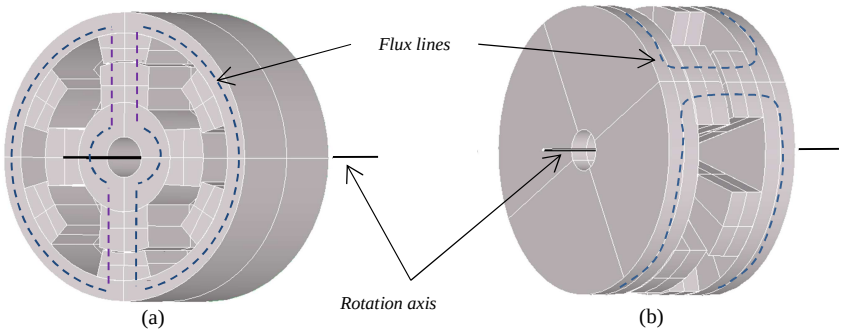

Fig. 1 SRM structures, (a) radial SRM, (b) axial SRM

2.1. ASRM with Single-Stator and Single-Rotor

The first category has a single stator and a single rotor (cf. Fig. 2 a); therefore, it has a single airgap. In this category, the axial magnetic force is unbalanced and important. For this reason, a robust guiding of the rotor is necessary. In [14], a 6/4 and 2.7 kW motor is presented. Due to the unbalanced axial force, the motor was not tested in its rated speed because "the rotor teeth hit to the stator teeth".

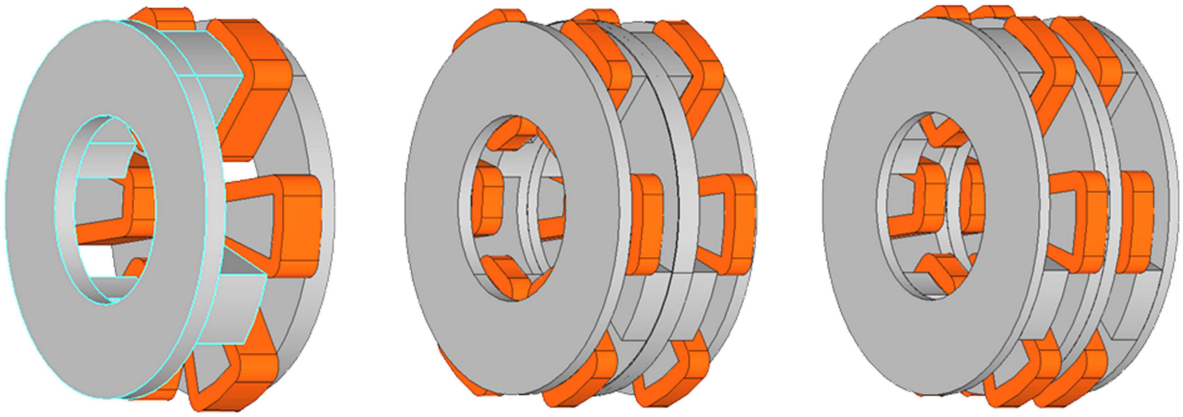

(a) (b) (c)

Fig. 2 ASRM categories, (a) ASRM with single-stator and single-rotor , (b) ASRM with double-stator and single-rotor, (c) ASRM with single-stator and double-rotor

2.2. ASRM with Double-Stator and Single-Rotor

In this configuration, the motor comprises a single rotor between two stators (Fig. 2 b), so the motor has two airgaps. The main advantage is that the axial forces are balanced. Indeed, the axial force of each stator on the rotor is compensated with the force of the other stator. The torque ripples can be reduced by an angular shift of stators [15]. However, this shift may cause unbalanced axial forces. In patent [1], the inventor presents this structure and uses the rolling method for the motor lamination. This lamination requires a variable pitch between the teeth in order to use a rolling process. Although, the study is poorly detailed in this patent, the inventor announces several advantages namely the reduction of torque ripples, noise, vibrations and iron losses… Additionally, the inventor does not propose the solution to hold rotor teeth if the rotor yoke is removed. In [16], authors highlight some acoustic advantages of this structure.

2.3. ASRM with Single-Stator and Double-Rotor

This configuration has a single stator and two external rotors (cf. Fig. 2 c). The position of stator in the middle leads to a complicated cooling. In the patent [17], inventors explain, without calculations, how to adapt radial concept of SRM into axial concept with double rotor. However, the use of global coils complicates the insertion of winding, and consequently increases the cost of the machine. In addition, this patent does not provide a detailed study to verify the announced benefits, like: “high efficiency with lower copper loss; improved thermal performance; lower torque ripple; higher torque density and lower costs for mass production”. Authors of [18] have used this motor for automotive traction. ASRM with segmental rotor for traction wheel is used in [19] and [20]. In [19], authors propose an original shift which reduces the torque ripples without unbalancing the axial forces. In [20], the machine has more teeth in the rotor than in the stator in order to increase the torque density.

3. PRESENTATION OF THE STUDIED AXIAL MACHINE

In this part, the work about the ASRM are presented for an electric vehicle application.

3.1. Choice of Axial Typology and Configuration

Double saliency axial switched reluctance motor with single rotor placed between two stators is chosen for our works (Fig. 2.b; Fig. 3.a). This structure is essentially selected because of the possibility to use local or transverse magnetic field loops depending on the coil winding direction (Fig. 3.b.c), compensation of axial forces on the rotor, possibility to reduce torque ripples by stators shifting [6] and easy cooling. Moreover, the two stators are mechanically joined, giving better mechanical behaviour. In other words, the axial forces

are compensated. In addition, a concentrated winding is here used in order to reduce copper losses. Each phase comprises eight coils which are connected as in "Fig 3-d" (serial - parallel).

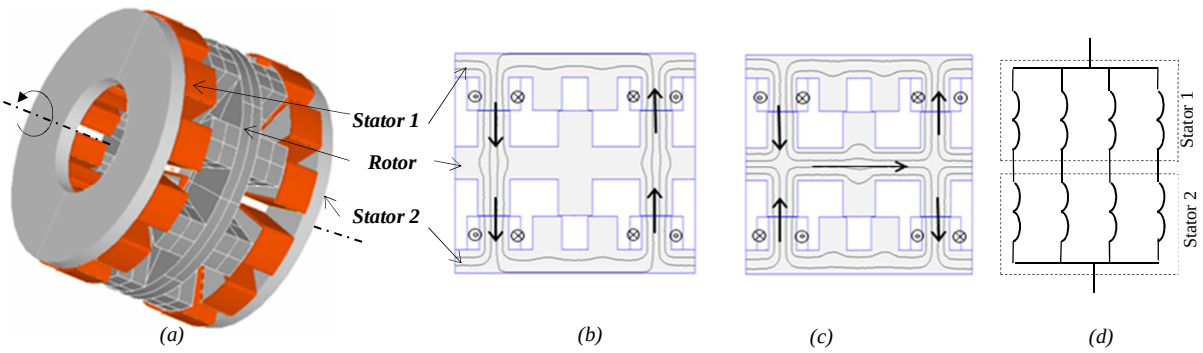

Fig. 3 (a) chosen SRM, (b) cross sectional view of transverse loops, (c) cross sectional view of local loops, (d) phase coils connection

For confidentiality reasons, the values of the different variables, including rotor position, are normalized with respect to the RSRM one, throughout all this work. Furthermore, the dimensions and characteristics of motors are not given for the same reasons.

3.2. ASRM Modelling

A half of the chosen axial motor is firstly drawn in 3D and meshed with Plateform Salome software [21]. The computed mesh (cf. Fig. 4) comprises 388920 tetrahedrons, 15136 prisms and 84578 nodes. This mesh is then exploited in an electromagnetic calculation code "*code_Carmel_3D*" of L2EP laboratory (Laboratoire d'électrotechnique et d'électronique de puissance de Lille) [22]. This code is used for the establishment of ASRM features: torque, flux linkage and axial force as function of rotor position and current.

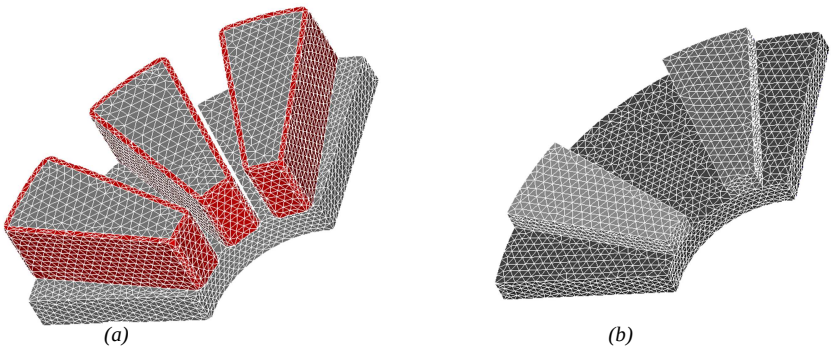

Fig. 4 ASRM mesh, (a) 1/4 stator mesh, (b) 1/4 rotor mesh

"*Code_Carmel_3D"* is used here for 3D finite element magnetostatic calculations with help of the *overlapping* finite element method [23], which allows to take into account the rotor displacement. The formulation is based on scalar potential Ω and magnetic source field H_s (equation (1)). Therefore, conjugate gradient method is used to solve the problem. The torque is then calculated with virtual work principle.

$$H = H_s - grad\ (\Omega) \qquad (1)$$

In order to compute the magnetic ASRM characteristics (torque, flux ...), only one phase is supplied by constant current and the rotor moves from an unaligned position to an aligned one.

To understand and highlight the advantages, disadvantages and characteristics of the axial machine, a comparative study is carried out with a radial machine. Therefore, a prototype of RSRM is used as a reference to design the ASRM. In this work, some passage rules from radial SRM to axial one are established in the next parts.

4. PASSAGE FROM RSRM TO ASRM AT SAME VOLUME

Passage rules are developed to transform a reference RSRM into an equivalent ASRM. The radial one is a prototype designed for an electric vehicle. Thus, this prototype has been designed in order to meet the requirements of powertrain specifications.

In this part, the ASRM is designed to take up the same volume as the radial one, i.e. the ASRM has the same diameter and the same length as the RSRM. So, some motors features are considered identical, such as typology (number of poles and phases), material (in the stator and in the rotor), airgap length, axial length, extern radius, current density, specific electric loading, maximum current, DC voltage and arc poles (see Fig. 5, example $\beta_s=\beta_{sr}$).

As mentioned, the external radius and the axial length are the same in order to have the same volume (*equations (*2*) and (*3*)).*

$$De=D_S \qquad (2)$$

$$L_{axi}=L_{rad} \qquad (3)$$

where d_e is the extern diameter of ASRM, D_s is the extern diameter of RSRM, L_{axi} is the axial length of ASRM and L_{axi} is the radial length of ASRM.

The determination of external diameter gives several choices of the inner diameter of the ASRM (d_i), which affects several ASRM dimensions. Thus, to choose the inner diameter (d_i), a compromise has to be done. In one hand, a small inner diameter (d_i) makes the distance "*e*" (cf. Fig. 5-b) between two stator poles very small and hence the slots are very narrow to place the coils. Moreover, a small inner diameter increases the stator pole section "S_{ds}" (cf. Fig. 5), and so, the yoke section "S_{cs}" must be increased also. The reason is linked to the fact that the two sections are crossed by the same flux. These last increases can lead

to a longer axial structure. On the other hand, a great inner diameter reduces airgap surface which decreases the developed torque. In order to mount the coils on the teeth, a sufficient space is necessary for the slots without increasing axial length, here the chosen value is *0.45* D_S.

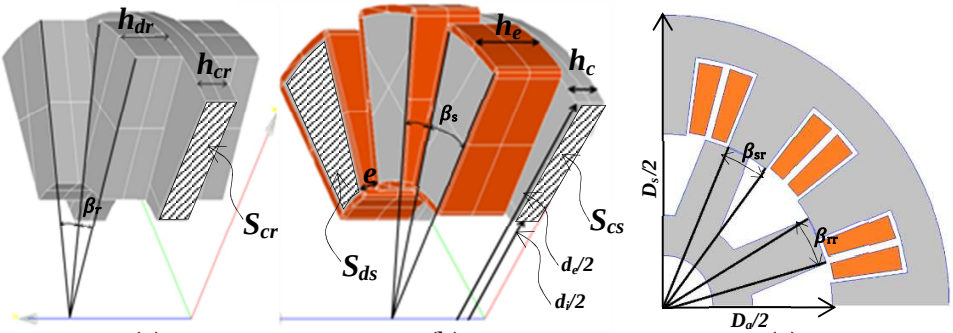

(a) (b) (c)

Fig. 5 (a, b) ASRM dimensions, (c) RSRM dimensions

To keep the same specific electric loading, the number of turns of the ASRM "n_a" is computed by using the RSRM turns number "n_r". According to Krishnan [24], the specific electric loading of radial SRM is defined as in the equation (4).

$$A_{rad} = \frac{2n_{ph}I}{D_a\pi} \qquad (4)$$

With the same approach, the electric loading of our axial machine (A_{ax}) can be computed (the bore diameter (D_a) is substituted by a quadratic diameter (d_q)):

$$A_{ax} = \frac{2n_{ph}I}{d_q\pi} \qquad (5)$$

with $d_q = \sqrt{(d_e^2 + d_i^2)/2}$

So

$$n_a = D_a / d_q \cdot n_r \qquad (6)$$

4.1. Choice of Transverse or Local Loops

Considering that the selected structure can use local or transverse loops, the developed torques of each loop are compared (Fig. 6). To make this comparison, one phase is powered by a constant current and the rotor rotates from the unaligned to the aligned position. Two currents are considered in order to see the influence of magnetic saturation.

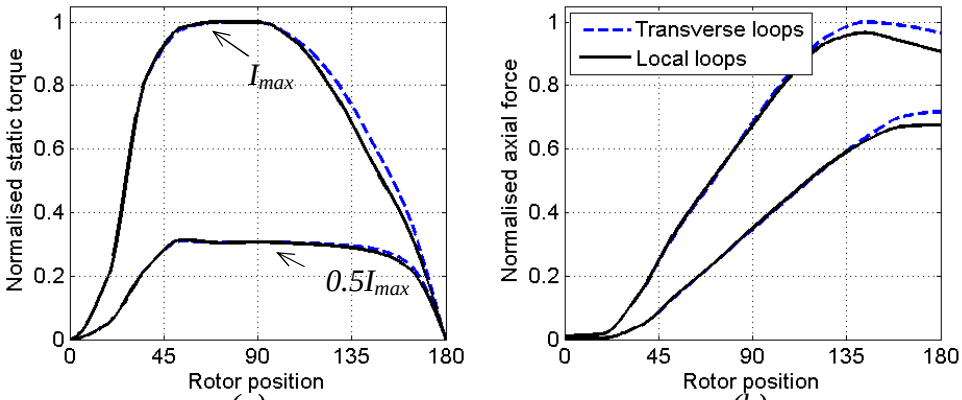

(a) *(b)*

Fig. 6 Torques and axial forces of one stator ASRM

The average torque is higher in the transverse configuration than in the local configuration with an average increase of 2.25% (Fig 6-a). At low current, the difference is negligible, but significant difference appears with the increasing of supply current. This difference is more important near the aligned position (between 100° and 180°).

The figure (Fig 6-b) presents the resultant axial forces applied by a single stator on the rotor. Their behaviour seems similar to the behaviour of the torque. Indeed, the difference between the two configurations is also more noticeable near the aligned position and at high current. These differences are due to the rotor yoke saturation near the aligned position.

Indeed, this yoke is fully crossed by flux in the local configuration unlike in the transverse one (Fig 3-b-c). This saturation limits the flux in the local loop configuration reducing the inductance value in this position and consequently reduces the inductances ratio. For the rest of this work, only transverse configuration is considered because of its average torque values (+2.25% on average).

4.2. Comparison of ASRM and RSRM at Same Volume

In this part, finite element studies are performed to assess the ASRM and to compare it to the RSRM. The static torque and the flux are first compared (Fig. 7). Two currents are considered.

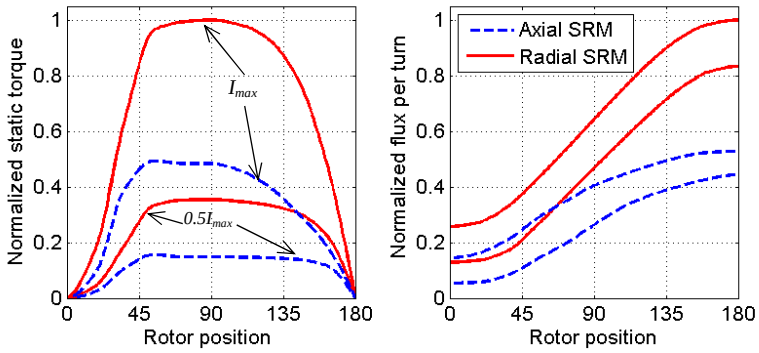

Fig. 7 Static torque and flux per turn

In all cases of comparison, the radial machine develops more torque than the axial one when the same volume is considered. At the same excitation current, the difference can reach 52%. Similar differences as in torque comparison are found when comparing the flux. For a given current, there is more flux in the RSRM than in the ASRM, whatever the rotor position is. These differences are mainly due to:

- The use of double stators while keeping the same mechanical airgap length. This automatically increases the magnetic airgap length. Indeed, a field line crosses the airgap two times in the RSRM but four times in the axial one,

- In electrical machines, airgap is known as the region where the magnetic energy is concentrated. The airgap area is greater in the radial machine than in the axial one (+10 %),

- The flux cross-section (stator pole area) is higher in the RSRM by 55%; which has a direct effect on the inductances.

The ASRM is less heavy than the radial one (20% of reduction), in addition, it uses less copper (43 %) and less iron (17 %). Furthermore, the torques densities, namely the maximum torque per the total weight and the maximum torque per the copper mass, are more important respectively by 37% and 15% in ASRM

5. PASSAGE FROM RSRM TO ASRM AT SAME TORQUES

This part concerns a design of the ASRM to fulfil similar torque specifications as the radial one.

5.1. Pre-Design Equation of Radial SRM

The reference [24] gives a pre-design equation of SRM similar to those of conventional machines. This equation gives the torque as a function of some machine parameters.

$$T = \eta(1-\lambda)B.A_{rad}\pi\left(\frac{D_a}{2}\right)^2 L \qquad (7)$$

Where T is the torque, η is the efficiency, λ is the inductances ratio, B is the airgap magnetic density, A_{rad} is the specific electric loading, L is the axial length and I is the current amplitude.

In this equation, several machine parameters appear, in particular, the airgap volume. Indeed, the torque depends on bore radius (D_a) and the length of the machine called "active length". Furthermore, the torque depends on the magnetic density in the airgap, the ratio of inductances and the specific electric loading. The reader can refer to the reference [24] for more information. The last parameter is chosen according to the cooling and to the maximum number of turns. It must be determined for a given current.

5.2. Pre-Design Equation of the Axial SRM

Similarly to Krishnan approach [24], a pre-design equation of the ASRM is here proposed.

$$T = \eta(1-\lambda)BA_{ax}\frac{1}{2}\pi\left(\frac{d_e^2 - d_i^2}{4}\right)\left(\frac{d_e + d_i}{4}\right) \qquad (8)$$

The ASRM torque depends directly on mean radius "$(d_i+d_e)/4$", the area of a single airgap, magnetic induction and inductances ratio. Unlike the RSRM, the axial length of the ASRM does not appear in this equation. So, the torque is directly independent of the axial length (if we do not take into account the influence of this variable into the magnetic saturation).

5.3. *Identification of the Pre-Design Equations*

As mentioned, the purpose of this conversion is the rapid design of ASRM. Thus, it is considered that the specifications of the axial machine are the same as the radial one. In addition, some assumptions are adopted. The motors have the same features like: efficiency, induction in the airgap, inductances ratio and specific electric loading. Furthermore, a constraint on axial length is considered, i.e. the machines must have the same axial length. Seen that the inner diameter *(d_i)* is limited by the slot area, there is only a choice for outer diameter *(d_e)*. By identification of the two pre-design equations, we obtain the next passage equation:

$$\frac{1}{8}\left(d_e^2 - d_i^2\right)\cdot\left(d_e + d_i\right) = D_a^2 L \qquad (9)$$

Several values of {*di, de*} give an equivalent ASRM to the reference RSRM. So, if d_i is known, the equation (9) has three solutions, two imaginary numbers (not acceptable) and one that is real.

5.4. *Comparison between ASRM and RSRM at the Same Torques*

In order to limit the volume, the values of {*di, de*} are chosen to give the minimum volume. As mentioned above, the inner diameter (*di*) was chosen to have a sufficient space in the slot which allows housing coils (*di=0.45 Ds*). Once the inner diameter is determined, the extern diameter is computed by solving analytically the equation (9) (*de=1.2 Ds*).In others words, to have the same torque, the volume of the axial machine must be increased and the number of turns must also be increased from $1.3n_r$ to $1.55n_r$ (cf. equation 6).

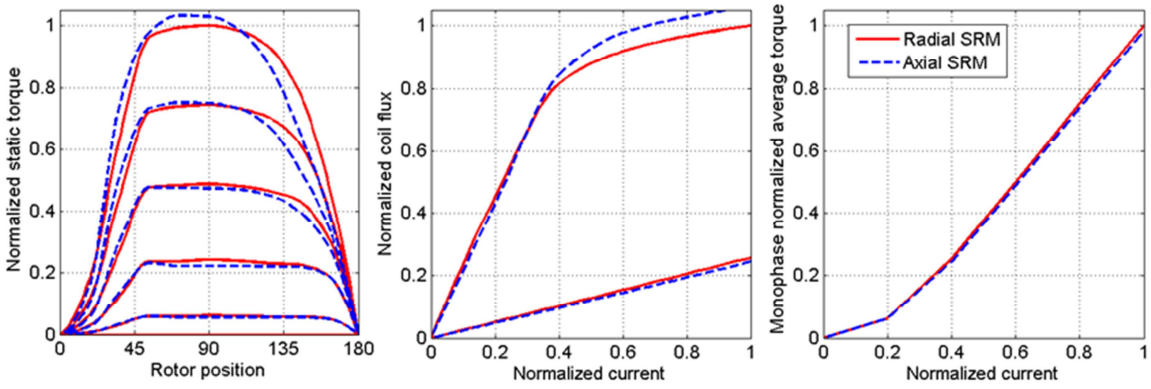

(a) *(b)* *(c)*

Fig. 8(a) Static torques, (b) flux linkages, (c) average torques

The 3D computations show that the new axial machine can reach the torque of the radial one, whatever the considered current (Fig. 8.a and Fig. 8.c). The linkage flux is almost the same for both (Fig. 8.b), so they should have the same envelope curve. Indeed, the torque is directly related to conversion surface of energy which is delimited by flux linkage and magneto-motive force (MMF, *nI*).

The increase of extern diameter affects directly the ASRM mass; this is why the axial SRM is here heavier than the radial one (about +23 %). However, ASRM develops the same torque as its rival with less amount of copper (-8%). Concerning the torque densities, the maximum torque per the total mass is better in the RSRM (+23%), but the maximum torque per the copper mass is better in the ASRM (+8.5 %).

The increase in ASRM mass presents a disadvantage for this SRM. To remedy this problem, we propose to remove the rotor yoke which has no electromagnetic interest (transverse loops are here used). After this modification, the masses of magnetic structures are almost the same (+2.6%). In addition, less copper is used in the axial machine (-8.4%).Thus, ASRM can compete with the RSRM because of only -2.5% deficit in ratio of

the torque per the total mass. For the ratio of the torque per copper mass, the axial motor is still better (+8.5%).The fact of removing the rotor yoke allows also reducing the axial length of ASRM by 16%. However, this might complicate the rotor teeth fixation and then the motor manufacturing.

5.5. Comparison at Operating Mode

In this comparison, speed-torque curves and corresponding torque ripples of the two machines are considered (cf. Fig. 9). In automotive applications, one of the specifications is the compliance to a defined torque-speed-curve. Last is defined as the maximum average torque developed when the machine is supplied by the maximum current and the maximum voltage for given speed [25]. The optimization of the control angles is taken into account by our software "*MRVSIM*"[26]. *MRVSIM* is a calculation code under MATLAB® used for the design of radial SRM. This tool uses analytical and/or numerical model of SRM and its control parameters optimization takes into account the machine and the associated converter. First, finite element model is employed for accurate computation of cartographies (flux and torque as function of current supply and position). By exploiting these features and by optimizing the turn-on and turn-off angles, the torque-speed curve of SRM can be calculated.

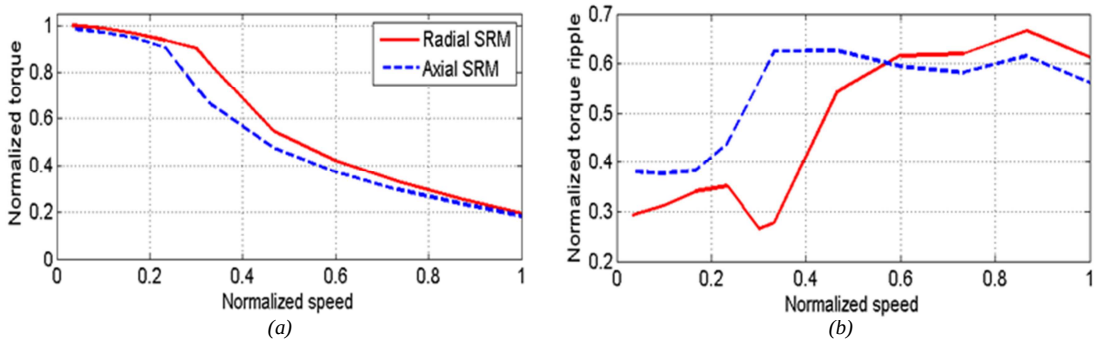

Fig. 9 (a) Maximum torque vs. speed curves, (b) torque-ripple vs. speed curves

By increasing the motors speeds, the electromotive force (EMF) increases and limits the supply current that reduces thus the average torque for both machines. At low speed, the two machines develop almost the same torque (-2%). Indeed, the equation passage was established in static mode with constant current and these conditions are observed when the motor is operating at low speed. Nevertheless, when increasing the speed, the RSRM develops more torque compared to ASRM, in particular near the rated speed, where the difference can reach -20%. Besides this, the RSRM is more suitable to this specific point which is the rated speed than the axial one, because the first one was directly designed and sized for this point. At high speed, the EMF prevents to achieve the reference currents in the two SRM. In this operating range, the difference between the torques is low, because the two SRM have almost the same coils flux, which is directly related to EMF.

According to the torque ripples (Fig. 9.b), no SRM can be considered advantageous for all speed range. So, the minimum torque ripple cartographies are computed in the next part (cf. Fig. 10). These cartographies consist to look for the optimal control parameters that allow minimum torque ripples across the entire operating range [27].

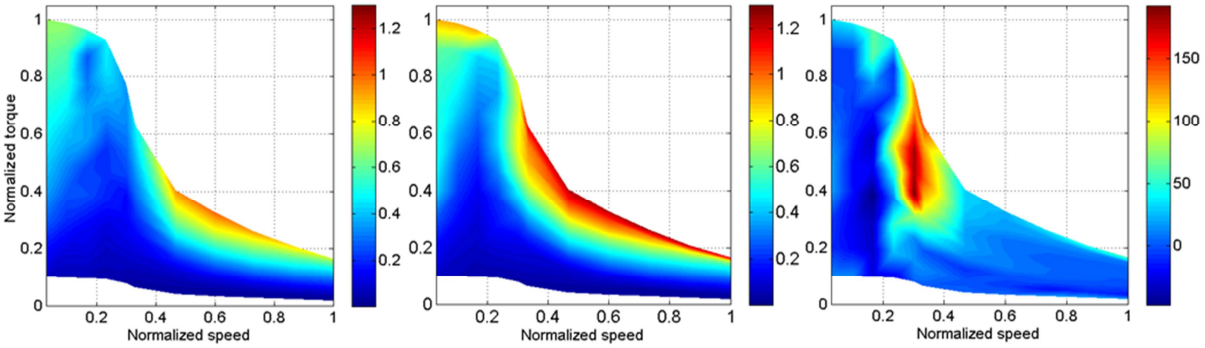

Fig. 10 Cartographies with minimum torque ripples, (a) RSRM (b) ASRM, (c) Differences (ASRM minus RSRM [%])

The results of this comparison do not allow retaining one conclusion on the all entire operating range because those results change from an operating point to other. Nevertheless, it can be noticed that the axial machine has generally less ripples at low speeds. This can be considered as an advantage, because at these speeds, it is more difficult to mechanically filter ripples than at high speeds.

6. CONCLUSION

ASRM with double stator and single rotor has been chosen for automotive application. Equations to pass from the reference radial machine to the axial one have been detailed. Firstly, the passage was at same volume but it shows that ASRM cannot reach torque performances of RSRM. Secondly, the passage was at same torque, where the axial SRM had to satisfy the same specification as the radial one. For this, the extern radius has been increased. In this configuration, ASRM gives similar torque compared to RSRM with smaller copper volume. However, this axial SRM was heavier than the radial one. In order to have the same mass of magnetic structures, it was proposed to withdraw the rotor yoke.

Concerning the speed-torque curves, there was almost the same curve except around the rated speed. The study of the minimum torque ripple cartographies has shown that axial machine had less torque ripples at low speed, presenting here an advantage of this structure for EV application and comfort criterion.

This paper has proved that, despite some advantages presented by the axial SRM, the radial SRM seems finally to be the most adequate structure for the specifications in the automotive application. Indeed, the designed axial structure is not able to reach all operating points of the speed-torque curve, unlike the radial one. Furthermore, the mass and volume of axial machine are more important than in the case of the radial ones. The solution of axial SRM without rotor yoke limits these drawbacks, but also complicates the manufacturing. For all these reasons, it has been decided to stop the works on this axial structure without the prototype manufacture. Ongoing works will then focus on the design of the radial structure for electric vehicle motorization.

7. REFERENCES

[1] Y. Li and J. D. Lloyd, 'Axial flux reluctance machine with two stators driving a rotor', *USA, patent*, 20-Jul-1999.

[2] R. Madhavan and B. G. Fernandes, 'Comparative analysis of axial flux SRM topologies for electric vehicle application', in *2012 IEEE International Conference on Power Electronics, Drives and Energy Systems (PEDES)*, 2012, pp. 1–6.

[3] J. Ma, R. Qu, and J. Li, 'Optimal design of axial flux switched reluctance motor for electric vehicle application', in *2014 17th International Conference on Electrical Machines and Systems (ICEMS)*, 2014, pp. 1860–1865.

[4] H. Goto, S. Murakami, and O. Ichinokura, 'Design to maximize torque-volume density of axial-flux SRM for in-wheel EV', in *IECON 2015 - 41st Annual Conference of the IEEE Industrial Electronics Society*, 2015, pp. 005191–005196.

[5] S. Haghbin, A. Rabiei, and E. Grunditz, 'Switched reluctance motor in electric or hybrid vehicle applications: A status review', in *2013 8th IEEE Conference on Industrial Electronics and Applications (ICIEA)*, 2013, pp. 1017–1022.

[6] M. A. Cinar and F. E. Kuyumcu, ‘Design and Drives Simulation of an In-Wheel Switched Reluctance Motor for Electric Vehicle Applications’, in *2007 IEEE International Electric Machines Drives Conference*, 2007, vol. 1, pp. 50–54.
[7] K. Watanabe, S. Aida, A. Komatsuzaki, and I. Miki, ‘Driving force characteristics of 40kW switched reluctance motor for electric vehicle’, in *International Conference on Electrical Machines and Systems, 2007. ICEMS*, 2007, pp. 1894–1898.
[8] X. D. Xue, J. K. Lin, Z. Zhang, T. W. Ng, K. F. Luk, K. W. E. Cheng, and N. C. Cheung, ‘Study of motoring operation of in-wheel switched reluctance motor drives for electric vehicles’, in *3rd International Conference on Power Electronics Systems and Applications, 2009. PESA 2009*, 2009, pp. 1–6.
[9] S. P. Nikam, S. Sau, and B. G. Fernandes, ‘Design of switched reluctance motor based electric drive-train for intra-campus two wheeler’, in *IECON 2013 - 39th Annual Conference of the IEEE Industrial Electronics Society*, 2013, pp. 4612–4617.
[10] T. Ogasawara, H. Goto, and O. Ichinokura, ‘A study of rotor pole shape of in-wheel direct drive SR motor’, in *2013 15th European Conference on Power Electronics and Applications (EPE)*, 2013, pp. 1–7.
[11] J. D. Widmer, R. Martin, and B. C. Mecrow, ‘Optimisation of an 80kW Segmental Rotor Switched Reluctance Machine for automotive traction’, in *Electric Machines Drives Conference (IEMDC), 2013 IEEE International*, 2013, pp. 427–433.
[12] N. Ouddah, M. Boukhnifer, A. Chaibet, E. Monmasson, and E. Berthelot, ‘Experimental robust H #x221E; controller design of switched reluctance motor for electrical vehicle application’, in *2014 IEEE Conference on Control Applications (CCA)*, 2014, pp. 1570–1575.
[13] H. Cheng, H. Chen, and Z. Yang, ‘Average torque control of switched reluctance machine drives for electric vehicles’, *IET Electr. Power Appl.*, vol. 9, no. 7, pp. 459–468, 2015.
[14] H. Arihara and K. Akatsu, ‘A basic property of axial type Switched Reluctance Motor’, in *Electrical Machines and Systems (ICEMS), 2010 International Conference on*, 2010, pp. 1687–1690.
[15] M. J. Kermanipour and B. Ganji, ‘Modification in Geometric Structure of Double-Sided Axial Flux Switched Reluctance Motor for Mitigating Torque Ripple’, *Can. J. Electr. Comput. Eng.*, vol. 38, no. 4, pp. 318–322, Fall 2015.
[16] F. Daldaban and N. Ustkoyuncu, ‘New disc type switched reluctance motor for high torque density’, *Energy Convers. Manag.*, vol. 48, no. 8, pp. 2424–2431, Aug. 2007.
[17] P. C. Desai, A. Emadi, and U. Krishnamurthy, ‘Switched Reluctance Machine’, *USA, patent*, 2011.
[18] H. Goto, T. Shibamoto, K. Nakamura, and O. Ichinokura, ‘Development of high torque density axial-gap switched reluctance motor for in-wheel direct-drive EV’, presented at the 2013 15th European Conference on Power Electronics and Applications (EPE), 2013, pp. 1–7.
[19] R. Madhavan and B. G. Fernandes, ‘A Novel axial flux segmented SRM for electric vehicle application’, in *Electrical Machines (ICEM), 2010 XIX International Conference on*, 2010, pp. 1–6.

[20] R. Madhavan and B. G. Fernandes, ‘Axial Flux Segmented SRM With a Higher Number of Rotor Segments for Electric Vehicles’, *IEEE Trans. Energy Convers.*, vol. 28, no. 1, pp. 203–213, 2013.
[21] ‘http://www.salome-platform.org/’. .
[22] Y. Le Menach, S. Clénet, and F. Piriou, ‘Determination and utilization of the source field in 3D magnetostatic problems’, *IEEE Trans. Magn.*, vol. 34, no. 5, pp. 2509–2512, 1998.
[23] H. Zaidi, L. Santandrea, G. Krebs, Y. Le Bihan, and E. Demaldent, ‘Use of Overlapping Finite Elements for Connecting Arbitrary Surfaces With Dual Formulations’, *IEEE Trans. Magn.*, vol. 48, no. 2, pp. 583–586, Feb. 2012.
[24] R. Krishnan, *Switched reluctance motor drives: modeling, simulation, analysis, design, and applications*. CRC, 2001.
[25] M. Rekik, M. Besbes, C. Marchand, B. Multon, S. Loudot, and D. Lhotellier, ‘High-speed-range enhancement of switched reluctance motor with continuous mode for automotive applications’, *Eur. Trans. Electr. Power*, vol. 18, no. 7, pp. 674–693, 2008.
[26] M. Besbes and B. Multon, ‘MRVSim code : Logiciel de simulation pour l’aide au dimensionnement des MRVDS et de convertisseur’, IDDN.FR.001.430010.000.S.C.2004.000.30645, 2004.
[27] A. Kolli, G. Krebs, X. Mininger, and C. Marchand, ‘Impact of command parameters on efficiency, torque ripple and vibrations for Switched Reluctance motor’, presented at the 2012 XXth International Conference on Electrical Machines (ICEM), 2012, pp. 2975–2980.